LHC would-be $\gamma\gamma$ excess as a nonperturbative effect of the electroweak interaction

Boris A. Arbuzov* and Ivan V. Zaitsev

Skobeltsyn Institute of Nuclear Physics, Lomonosov Moscow State University, Leninskie gory 1, 119991 Moscow, Russia

(Received 22 February 2012; revised manuscript received 29 March 2012; published 4 May 2012)

The recently reported would-be excess at 125 GeV in invariant mass distribution of $\gamma\gamma$ and of $l^+l^+l^-l^-$ obtained in the course of the Higgs boson search at LHC is tentatively interpreted as a scalar bound state of two W. Nonperturbative effects of electroweak interactions obtained by the application of the Bogoliubov compensation approach lead to such bound states due to the existence of anomalous three-boson gauge-invariant effective interactions. The application of this scheme gives satisfactory agreement with existing data without any adjusting parameter except for the bound state mass 125 GeV, while σBR for $\gamma\gamma$ resonance is predicted to be twice as much as the value for the standard model Higgs. The decay channel γl^+l^- and an effect in 3γ production may serve as decisive checks of the interpretation.

DOI: 10.1103/PhysRevD.85.093001 PACS numbers: 12.15.−y, 12.15.Ji, 14.70.Fm, 14.80.Ec

I. STRONG EFFECTIVE TREE-BOSON INTERACTION

Recent LHC results on searches for Higgs [1,2] already induce active discussions. Hints on the existence of a state with mass around 125 GeV, which manifests itself in decays to $\gamma\gamma$ and $l^+l^+l^-l^-$, are interpreted not only in terms of the standard model (SM) Higgs, but also in different variant extensions of the SM: fermiophobic Higgs [3], two Higgs doublet models [4], etc. In any case data being presented in [1,2] allow the discussion of different options, as agreement of the data with SM predictions is not very convincing.

In the present work we will discuss an interpretation of the would-be LHC 125 GeV bump in terms of nonperturbative effects of the electroweak interaction. For this purpose, we rely on an approach induced by the N. N. Bogoliubov compensation principle [5,6]. In [7–13], this approach was applied to studies of a spontaneous generation of effective nonlocal interactions in renormalizable gauge theories. In particular, papers [12,13] deal with an application of the approach to the electroweak interaction and a possibility of the spontaneous generation of an effective anomalous three-boson interaction of the form

$$\begin{aligned} &-\frac{G}{3!}F\epsilon_{abc}W^a_{\mu\nu}W^b_{\nu\rho}W^c_{\rho\mu},\\ &W^3_{\mu\nu}=\cos\theta_W Z_{\mu\nu}+\sin\theta_W A_{\mu\nu},\\ &W^a_{\mu\nu}=\partial_\mu W^a_\nu-\partial_\nu W^a_\mu+g\epsilon_{abc}W^b_\mu W^c_\nu, \end{aligned} \tag{1}$$

with the uniquely defined form factor $F(p_i)$, which guarantees the effective interaction (1) acting in a limited region of the momentum space. This was done of course in the framework of an approximate scheme, whose accuracy was estimated to be $\simeq 10\%$ [7]. The would-be existence of the effective interaction (1) leads to important nonperturbative effects in the electroweak interaction. This is usually called the anomalous three-boson interaction, and it has been considered for a long time on phenomenological grounds [14,15]. Note that the first attempt to obtain the anomalous three-boson interaction in the framework of the Bogoliubov approach was done in [16]. Our interaction constant G is connected with conventional definitions in the following way:

$$G=-\frac{g\lambda}{M_W^2}, \tag{2}$$

where $g\simeq 0.65$ is the electroweak coupling. The current limitations for parameter λ read [17]

$$\lambda=-0.016^{+0.021}_{-0.023},\qquad -0.059<\lambda<0.026(95\%\ \text{C.L.}). \tag{3}$$

Interaction (1) increases with increasing momenta p. For the estimation of an effective dimensionless coupling we choose symmetric momenta (p, q, k) in a vertex corresponding to the interaction

$$\begin{aligned} &(2\pi)^4G\epsilon_{abc}(g_{\mu\nu}(q_\rho pk-p_\rho qk)+g_{\nu\rho}(k_\mu pq-q_\mu pk)\\ &\quad+g_{\rho\mu}(p_\nu qk-k_\nu pq)+q_\mu k_\nu p_\rho-k_\mu p_\nu q_\rho)\\ &\quad\times F(p,q,k)\delta(p+q+k)+\ldots, \end{aligned} \tag{4}$$

where p,μ,a; q,ν,b; k,ρ,c are, respectfully, incoming momenta, Lorentz indices, and weak isotopic indices of W bosons. We also mean that there are four-boson, five-boson and six-boson vertices present according to the expression for $W^a_{\mu\nu}$ (1). In what follows we shall use the four-boson vertex, which corresponds to the following interaction:

$$\Delta L=\frac{gG}{2}\epsilon_{abc}\epsilon_{aed}W^e_\mu W^d_\nu W^b_{\nu\rho}W^c_{\rho\mu}. \tag{5}$$

The explicit expression for the corresponding vertex is presented in [12]. The form factor $F(p,q,k)$ is obtained in [13] using the following approximate dependence on the three variables:

*arbuzov@theory.sinp.msu.ru

$$F(p, q, k) = F\left(\frac{p^2 + q^2 + k^2}{2}\right). \tag{6}$$

The symmetric condition means

$$pq = pk = qk = \frac{p^2}{2} = \frac{q^2}{2} = \frac{k^2}{2} = \frac{x}{2}. \tag{7}$$

Interaction (1) increases with increasing momenta p and corresponds to the effective dimensionless coupling being of the following order of magnitude:

$$g_{\rm eff} = \frac{|g\lambda| p^2}{2M_W^2} F\left(\frac{3p^2}{2}\right). \tag{8}$$

The form factor $F(x)$ in [13] is expressed in terms of the Meijer functions [18]

$$\begin{aligned} F(z) = {} & \frac{1}{2} G_{15}^{31}\left(z\Big|^{0}_{1,1/2,0,-1/2,-1}\right) \\ & - \frac{85 g_0 \sqrt{2}}{128\pi} G_{15}^{31}\left(z\Big|^{1/2}_{1,1/2,1/2,-1/2,-1}\right) \\ & + C_1 G_{04}^{10}(z|1/2, 1, -1/2, -1) \\ & + C_2 G_{04}^{10}(z|1, 1/2, -1/2, -1), \\ z = {} & \frac{G^2 (p^2)^2}{512\pi^2}, \end{aligned} \tag{9}$$

$$g_0 = 0.6037, \qquad C_1 = -0.0351, \qquad C_2 = -0.0511, \tag{10}$$

where g_0 is the value of the electroweak running coupling at momentum p_0 corresponding to value of variable z,

$$z_0 = 9.6175. \tag{11}$$

Thus, the running coupling $g_{\rm eff}$, dependent on the variable $t = Gp^2$, is the following:

$$g_{\rm eff}(t) = \frac{t}{2} F\left(\frac{9t^2}{2048\pi^2}\right), \qquad t = Gp^2. \tag{12}$$

The behavior of $g_{\rm eff}(t)$ is presented in Fig. 1. We see that for $t \simeq 22$ the coupling reaches a maximal value $g_{\rm eff} = 3.63$; the corresponding effective α is the following:

$$\alpha_{\rm eff} = \frac{g_{\rm eff}^2}{4\pi} = 1.049. \tag{13}$$

Thus, for sufficiently large momentum, interaction (1) becomes strong and may lead to physical consequences analogous to that of the usual strong interaction (QCD). In particular, bound states and resonances consisting of W-s (W-hadrons) may appear. We have already discussed the possibility to interpret the would-be CDF Wjj excess [19] in terms of such a state [20].

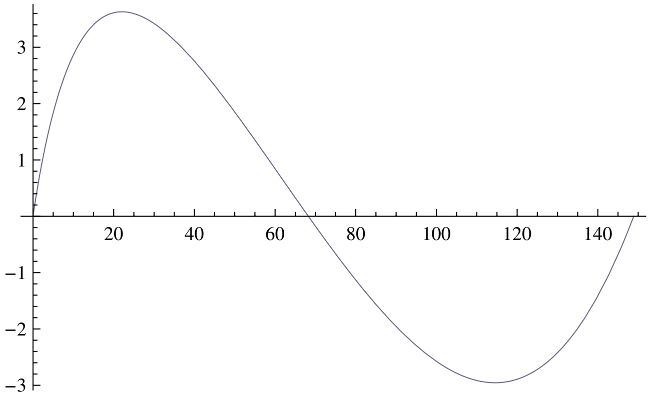

FIG. 1 (color online). Behavior of the effective coupling $g_{\rm eff}(t)$, $t = Gp^2$; $g_{\rm eff}(t) = 0$ for $t > 148$.

II. SCALAR BOUND STATE OF TWO W-s

In the present work we apply these considerations, along with some results of [13], to data indicating a possible excess in $\gamma\gamma$ and $l^+ l^+ l^- l^-$ production at the LHC [1,2] in the region of invariant mass, 120–130 GeV.

Let us assume that this excess is due to the existence of the bound state X of two W's with mass M_s. This state X is assumed to have spin 0 and also weak isotopic spin 0. Then, the vertex of the XWW interaction has the following form:

$$\frac{G_X}{2} W^a_{\mu\nu} W^a_{\mu\nu} X \Psi_0, \tag{14}$$

where Ψ_0 is a Bethe-Salpeter (BS) wave function of the bound state. Again, due to gauge invariance there is also a three-boson term

$$- g G_X \epsilon_{abc} W^a_{0\mu\nu} W^b_\mu W^c_\nu X, \tag{15}$$

as well as a four-boson term. In what follows we use expressions (14) and (15). The main interactions forming the bound state are just nonperturbative interactions (1) and (14). This means that we take into account the exchange of the vector boson W as well as of scalar bound state X itself. In diagram form the corresponding Bethe-Salpeter equation is presented in Fig. 2. We expand the kernel of the equation in powers of M_W^2 and M_s^2 and obtain the following equation with the introduction of a more suitable variable:

$$z = \frac{G^2 (p^2)^2}{64\pi^2}, \qquad t = \frac{G^2 (q^2)^2}{64\pi^2},$$

where p is the external momentum and q is the integration momentum.

$$
\begin{aligned}
\Psi_0(z) = {} & 4\int_0^{z_0'}\Psi_0(t)dt - \frac{2}{3z}\int_0^z \Psi_0(t)tdt + \frac{4}{3\sqrt{z}}\int_0^z \Psi_0(t)\sqrt{t}dt + \frac{4\sqrt{z}}{3}\int_z^{z_0'}\frac{\Psi_0(t)}{\sqrt{t}}dt - \frac{2z}{3}\int_z^{z_0'}\frac{\Psi_0(t)}{t}dt \\
& + \mu\Big(-\frac{1}{z}\int_0^z \Psi_0(t)\sqrt{t}dt + \frac{2}{\sqrt{z}}\int_0^z \Psi_0(t)dt + 6\int_0^{z_0'}\frac{\Psi_0(t)}{\sqrt{t}}dt + 2\sqrt{z}\int_z^{z_0'}\frac{\Psi_0(t)}{t}dt - z\int_z^{z_0'}\frac{\Psi_0(t)}{t\sqrt{t}}dt\Big) \\
& - \mu_s\Big(\frac{1}{8z\sqrt{z}}\int_0^z \Psi_0(t)tdt - \frac{25}{64z}\int_0^z \Psi_0(t)\sqrt{t}dt + \frac{19}{64\sqrt{z}}\int_0^z \Psi_0(t)dt + \frac{11}{8}\int_0^z\frac{\Psi_0(t)}{\sqrt{t}}dt + \frac{19}{16}\int_z^{z_0'}\frac{\Psi_0(t)}{\sqrt{t}}dt \\
& + \frac{5\sqrt{z}}{16}\int_z^{z_0'}\frac{\Psi_0(t)}{t}dt - \frac{5z}{64\sqrt{z}}\int_z^{z_0'}\frac{\Psi_0(t)}{t\sqrt{t}}dt - \frac{z\sqrt{z}}{64}\int_z^{z_0'}\frac{\Psi_0(t)}{t^2}dt\Big) - \frac{\kappa}{12\pi}\Big(\frac{1}{2z}\int_0^z \Psi_0(t)\sqrt{t}dt \\
& + \frac{3}{2\sqrt{z}}\int_0^z \Psi_0(t)dt + \frac{3}{2}\int_z^{z_0'}\frac{\Psi_0(t)}{\sqrt{t}}dt + \frac{\sqrt{z}}{2}\int_z^{z_0'}\frac{\Psi_0(t)}{t}dt\Big) + \frac{g}{4\pi}\Big(-\frac{1}{z}\int_0^z \Psi_0(t)\sqrt{t}dt \\
& + \frac{3}{\sqrt{z}}\int_0^z \Psi_0(t)dt + 3\int_z^{z_0'}\frac{\Psi_0(t)}{\sqrt{t}}dt - \sqrt{z}\int_z^{z_0'}\frac{\Psi_0(t)}{t}dt\Big), \\
\mu = {} & \frac{GM_W^2}{6\pi}, \qquad \mu_s = \frac{GM_s^2}{6\pi}, \qquad \kappa = \frac{G_X^2}{G}.
\end{aligned}
\tag{16}
$$

The upper line in the equation is the main (zero approximation) part. This line and terms proportional to μ^2 and μ_s^2 are obtained from the main triangle diagram (the second one in the upper line of Fig. 2) by expanding its expression in powers of $(M_W^2)^n$ and $(M_s^2)^n$. Then we take into account terms with $n = 0$, 1. Estimates show that higher powers can be neglected. The term proportional to κ, that is, to G_X^2, corresponds to the third diagram in the upper line of Fig. 2. Terms with gauge electroweak coupling g enter due to diagrams in the second line of Fig. 2. The upper limit z_0' is introduced for the sake of generality due to the experience of [7–13], according to which z_0' may be either ∞ or some finite quantity. That is, z_0' is defined in the process of solving the problem. The physical meaning of this parameter corresponds to the definition of the effective cutoff z_0', which bounds a "low-momentum" region, where the nonperturbative effects are significant. For the form factor of interaction (1), the upper limit z_0 (11) is defined in [13].

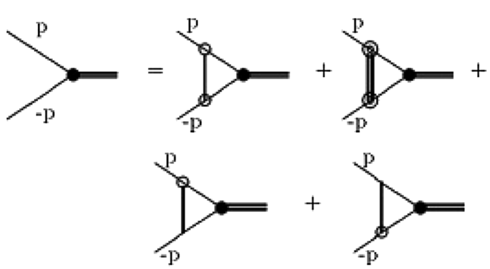

FIG. 2. Representation of the Bethe-Salpeter equation for W-W bound state. The black spots correspond to the XWW vertex (14) with the BS wave function. The empty circles correspond to the pointlike anomalous three-gluon vertex (1), and the double circle to the pointlike XWW vertex (14). The simple point is the usual gauge triple W interaction. The double line is the bound state X, and the single line is W.

The Bethe-Salpeter wave function in the first approximation is normalized by the condition $\Psi_0(0) = 1$, which corresponds to the following equality:

$$
4\int_0^{z_0'}\Psi_0(t)dt + \frac{2\sqrt{2}}{\pi}\int_0^{z_0}\frac{gF(t)}{\sqrt{t}}dt + \frac{3}{32\pi^2}\int_\mu^{z_0'}\frac{g^2\Psi_0(t)}{t}dt = 1, \tag{17}
$$

where $F(t)$ and z_0 are defined by Eqs. (9)–(12). In diagram form this condition is presented in Fig. 3. We also have to take into account the normalization condition for the Bethe-Salpeter wave function, which defines the interaction constant G_X. This condition guarantees the proper form of the effective propagator for bound state X. In diagram form it is presented in Fig. 4. Here each diagram is a coefficient before external momentum squared p^2; that is, for expression $\Phi(p^2, \ldots)$ we put

$$
\frac{\partial}{\partial p^2}\Phi(p^2, \ldots)|_{p^2=0}.
$$

Diagrams in Fig. 4 correspond to the following expressions:

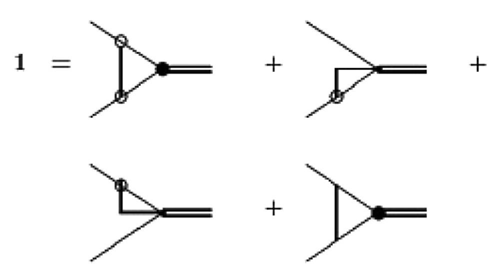

FIG. 3. Representation of the normalization condition $\Psi_0(0) = 1$. The four-leg vertex corresponds to interaction (15). All the external momenta are zero. Other notations are the same as in Fig. 2.

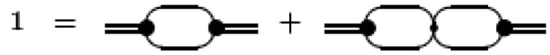

FIG. 4. Diagrams for the normalization condition of the XWW vertex. The four-leg vertex corresponds to vertex (5) being proportional to gG.

$$\frac{\kappa}{8\pi}\left(9I_0 - \frac{25}{16\pi}D^2\right) = 1, \qquad I_0 = \int_0^{z'_0} \frac{\Psi_1^2(z)dz}{\sqrt{z}}, \\ D = \int_0^{z'_0} \frac{\sqrt{g}\Psi_1(z)dz}{\sqrt{z}}. \tag{18}$$

We shall solve Eq. (16) by iterations. We take as the first approximation for the problem the set of equations consisting of

(i) the upper line of Eq. (16), that is, (16) with $\mu = \mu_s = \kappa = g = 0$;
(ii) condition $\Psi_0(0) = 1$ (17);
(iii) normalization condition (18) for the BS wave function.

There are a few solutions to the set of Eqs. (16) and (17), but only one of them leads to positive M_s^2. It reads

$$\Psi_1(z) = \frac{\pi}{2}G^{21}_{15}(z|^0_{1,0,1/2,-1/2,-1}) + C_1 G^{20}_0(z|_{1,1/2,-1/2,-1}) \\ + C_2 G^{10}_0(-z|_{1,1/2,-1/2,-1}), \\ z'_0 = 44.151\,234, \\ C_1 = 3.054\,37, \\ C_2 = -0.001\,196\,4. \tag{19}$$

where we again use Meijer functions [18]. Now we use the solution (19) and obtain the parameter κ (16) with the aid of the normalization condition for XWW coupling (18).

With Ψ_1 (19) we obtain from (18)

$$\kappa = 0.592\,411. \tag{20}$$

Then we multiply the full Eq. (16) by $\Psi_1(z)$ from the right and integrate the result by z in the interval $(0, z'_0)$. It is easy to see by changing the order in double integrals that all terms of zero order in μ, μ_s, κ, g vanish, and we have the following equation:

$$-\mu_s\left(\frac{3I_1}{64} - \frac{5I_2}{64} + \frac{95I_3}{64} + \frac{11I_4}{8} - \frac{I_5}{64}\right) \\ + \mu\left(-I_1 + 3I_2 + 14I_3 + 6I_4\right) - \frac{\kappa}{12\pi}(I_2 + 3I_3) \\ + \frac{3I_{g3} - I_{g2}}{4\pi} = 0, \tag{21}$$

where

$$I_1 = \int_0^{z'_0} \frac{\Psi_1(z)dz}{z\sqrt{z}} \int_0^z \Psi_1(t)t dt, \\ I_2 = \int_0^{z'_0} \frac{\Psi_1(z)dz}{z} \int_0^z \Psi_1(t)\sqrt{t}dt, \\ I_3 = \int_0^{z'_0} \frac{\Psi_1(z)dz}{\sqrt{z}} \int_0^z \Psi_1(t)dt, \\ I_4 = \int_0^{z'_0} \Psi_1(z)dz \int_0^z \frac{\Psi_1(t)dt}{\sqrt{t}}, \\ I_5 = \int_0^{z'_0} \frac{\Psi_1(z)dz}{z^2} \int_0^z \Psi_1(t)t\sqrt{t}dt, \\ I_{g2} = \int_0^{z'_0} \frac{g\Psi_1(z)dz}{z} \int_0^z \Psi_1(t)\sqrt{t}dt, \\ I_{g3} = \int_0^{z'_0} \frac{g\Psi_1(z)dz}{\sqrt{z}} \int_0^z \Psi_1(t)dt. \tag{22}$$

Now we define the running coupling g,

$$g = \frac{g(M_W)}{\sqrt{1 + \frac{5g^2(M_W)}{24\pi^2}\ \ln(1 + \frac{8\pi\sqrt{z}}{GM_W^2})}}. \tag{23}$$

It enters in integrals (20) and (22). We introduce $M_s = 125$ GeV, which means

$$\mu_s = \mu\frac{125^2}{80.4^2}, \tag{24}$$

and perform the necessary calculations. So we choose a solution with mean value $M_s = 125$ GeV from the ATLAS and the CMS results [1,2]; then we have a unique solution with the following parameters:

$$G_X = 0.000\,666\ \text{GeV}^{-1}, \qquad G = \frac{0.004\,84}{M_W^2}. \tag{25}$$

The result (25) is the parameter of the anomalous triple interaction (1), taking into account the relation (2),

$$\lambda = -\frac{GM_W^2}{g(0)} = -0.007\,44, \tag{26}$$

which doubtlessly agrees with the limitations (3).

III. COMPARISON TO EXPERIMENTS

Thus, we have scalar state X with coupling (14) and (25). In calculations of decay parameters and cross sections, we use the COMPHEP package [21]. We use the parameter G_X (25), obtained above from the BS wave function (19), and $M_s = 125$ GeV. The cross section of X production at the LHC with $\sqrt{s} = 7$ TeV reads

$$\sigma_X = \sigma(p + p \to X + \ldots) = 0.184\ \text{pb}. \tag{27}$$

Parameters of X decay are the following:

$$\Gamma_t(X) = 0.000502\ \text{GeV}, \quad \text{BR}(X \to \gamma\gamma) = 0.430,$$
$$\text{BR}(X \to \gamma Z) = 0.305, \quad \text{BR}(X \to 4l(\mu, e)) = 0.000577,$$
$$\text{BR}(X \to b\bar{b}) = 0.000024, \quad \text{BR}(X \to \gamma e^+ e^-) = 0.0231,$$
$$\text{BR}(X \to \gamma \mu^+ \mu^-) = 0.016, \quad \text{BR}(X \to \gamma \tau^+ \tau^-) = 0.0125,$$
$$\text{BR}(X \to \gamma u\bar{u}) = 0.0478, \quad \text{BR}(X \to \gamma c\bar{c}) = 0.0368,$$
$$\text{BR}(X \to \gamma d\bar{d}) = 0.0446, \quad \text{BR}(X \to \gamma s\bar{s})) = 0.0430,$$
$$\text{BR}(X \to \gamma b\bar{b}) = 0.0416. \tag{28}$$

For decay $X \to b\bar{b}$ we calculate the evident triangle diagram and use $m_b(125\ \text{GeV}) \simeq 2.9$ GeV. Branching ratios for decays to other fermion pairs are even smaller. We see that state X is quite narrow, so we would expect the observable width of the state to be defined by the corresponding experimental resolution.

Experimental data give, in the region of the would-be state, the following limitations for $\sigma_{\gamma\gamma} = \sigma_X \text{BR}(X \to \gamma\gamma)$:

$$\sigma_{\gamma\gamma} < 3.8\sigma(\text{SM}), \qquad \sigma_{\gamma\gamma} < 3.6\sigma(\text{SM}), \qquad \sigma_{\gamma\gamma} < 0.135\ \text{pb}. \tag{29}$$

Here $\sigma(\text{SM}) \simeq 0.04$ pb is the standard model value for the quantity under discussion, the upper line corresponds to ATLAS data [22], and the lower line correspond to CMS data [23]. First, both limitations are quite consistent. Second, our value for the same quantity from (27) and (28) reads

$$\sigma_{\gamma\gamma} = 0.077\ \text{pb} \tag{30}$$

which also agrees with limitations (29); however, it essentially exceeds the SM value $\sigma(\text{SM})$. At this point it is advisable to discuss the accuracy of our approximations. The former experience concerning both applications to the Nambu—Jona-Lasinio model in QCD [8,9,11] and to the electroweak interaction [12,13] shows that the average accuracy of the method is around 10% in values of different parameters. So we may assume that in the present estimations of the coupling constant G_X, we also have the same accuracy. For the cross section this means a possible deviation of up to 20% of the calculated value. Thus, we would change (30) to the following result:

$$\sigma_{\gamma\gamma} = (0.077 \pm 0.015)\ \text{pb}. \tag{31}$$

Branching ratios (28) do not depend on the value of G_X, so we assume their accuracy is considerably better than in (31). In any case result (31) agrees with (29).

There are also indications for some excess around 125 GeV in four-lepton states. With (27) and (28) we have, for the decay $X \to l^+ l^+ l^- l^- (l = \mu, e)$, $\sigma \times \text{BR} = (0.000\,11 \pm 0.000\,02)$ pb. For integral luminosity $L = 4.810^3\ \text{pb}^{-1}$ [22,23] we have, for the number of events,

$$N(4l) = \sigma \times \text{BR} \times L = (0.51 \pm 0.10), \tag{32}$$

i.e. close to one event. This result also essentially exceeds the SM expectations. As a matter of fact, ATLAS [24] has three events and CMS [25] has two in the region under consideration with the estimated background much smaller than one event. In any case our estimation (32) has no contradiction with data or the usual SM Higgs boson interpretation. In the future, more precise experiments at the LHC to determine the essential distinctions of our scheme and the SM Higgs boson variant could manifest themselves and decisively discriminate different variants. The distinctions refer to $\sigma_{\gamma\gamma}$ (31) and also to the four-lepton channel (32).

We emphasize the importance of channel $X \to \gamma l^+ l^-$. For this decay mode from (27) and (28) we predict

$$\sigma_X \text{BR}(X \to \gamma l^+ l^-) = (0.0073 \pm 15)\ \text{pb} \tag{33}$$

which gives $N = 35 \pm 7$ events for the already-achieved luminosity [1,2]. This channel may serve as an accurate test of our results because the SM value for quantity (33) gives around five events [26].

There is one point in the data [23] which provides hints against the SM option and, on the contrary, on behalf of our variant. The data of [23] deal with a two-jet tag, which singles out the channel of $X(H)$ production via vector boson fusion. We calculate the effect for this channel within our approach and obtain $\sigma_{\text{VBF}} = 0.079$ pb. Taking into account (28) and the efficiency in [23] for such a process as $\simeq 0.037$, we obtain six events of $\gamma\gamma$ decay of X, which by no means contradict CMS data [see [23], Fig. 1(b)]. The estimate for the SM Higgs gives less than one event here. Of course, there is no contradiction yet, but nevertheless, we may state a trend for better agreement with data of the present variant.

The main difference of our predictions with the SM results consists in the decay channel $X \to b\bar{b}$. For the SM Higgs, which is usually considered for the explanation of a would-be 125 GeV state, this decay is dominant, whereas our result (28) gives extremely small BR $\simeq 3 \times 10^{-5}$. We can emphasize that the SM Higgs interpretation could not proven unless the $b\bar{b}$ channel with the proper intensity is detected.

We can also draw attention to the quite promising process $pp \to \gamma + X + \ldots$ with $X \to \gamma\gamma$. Our option gives, for the process, the cross section $\sigma(\gamma, X \to 2\gamma + \ldots) \simeq 3.6$ pb at the LHC, which for the already-reached luminosity 4.8 fb^{-1}, gives around 17 events, whereas for the SM Higgs option the effect is negligible. This process could provide a decisive test of our proposal, especially as the amount of experimental data increases in the near future.

In considering consequences of the present results we have to keep in mind that the experimental evidence for a 125 GeV state is by no means decisive. If either the data [1,2] are not confirmed by forthcoming experiments or the SM Higgs interpretation of the state is proved, we may consider the possibility of applications of the results of the W-hadron model to searches for possible states X with other masses. As a matter of fact, the mass of the X state is defined by the value of the coupling constant (2) of interaction (1) with experimental limitations (3) for λ. The value $M_s = 125$ GeV corresponds to $\lambda = -0.0074$ (26). With $|\lambda|$ increasing, M_s also increases, and for the maximal admissible value $|\lambda| = 0.059$ (3), we have $M_s \simeq 920$ GeV. This means that if the application of our results to a would-be $M_s = 125$ GeV state fails for some reason, it might be advisable to look for X in the interval of masses up to 920 GeV. Of course, performance evaluations need to be done for values of M_s in the interval. Negative results of the search would decisively reject the possibility considered in the present work.

IV. CONCLUSION

Thus, we have an alternative interpretation of the LHC 125 GeV phenomenon. The overall data do not contradict the SM Higgs option or the scalar W-hadron, which we discuss here. However, our estimates of the effects are, as a rule, much larger than the SM Higgs predictions. It seems that data favor larger values. The forthcoming increase of the integral luminosity will undoubtedly discriminate these two options. If the future result is in favor of the scalar W-hadron, we need an additional comparison of our predictions with results of other possibilities, e.g. fermiophobic variants [27,28]. The application of this result to data [1,2] is discussed in [3].

ACKNOWLEDGMENTS

The authors express gratitude to E. E. Boos and V. I. Savrin for valuable discussions. The work was supported in part by Russian Ministry of Education and Science Grant No. NS-3920.2012.2.

[1] G. Aad *et al.* (ATLAS Collaboration), Phys. Lett. B **710**, 49 (2012); arXiv:1202.1408.
[2] S. Chatrchyan *et al.* (CMS Collaboration), Phys. Lett. B **710**, 26 (2012); arXiv:1202.1488.
[3] E. Gabrielli, B. Mele, and M. Raidal, arXiv:1202.1796.
[4] K. Blum and R. T. D'Agnolo, arXiv:1202.2364.
[5] N. N. Bogoliubov, Sov. Phys. Usp. **2**, 236 (1959).
[6] N. N. Bogoliubov, Physica (Amsterdam) **26**, S1 (1960).
[7] B. A. Arbuzov, Theor. Math. Phys. **140**, 1205 (2004).
[8] B. A. Arbuzov, Phys. At. Nucl. **69**, 1588 (2006).
[9] B. A. Arbuzov, M. K. Volkov, and I. V. Zaitsev, Int. J. Mod. Phys. A **21**, 5721 (2006).
[10] B. A. Arbuzov, Phys. Lett. B **656**, 67 (2007).
[11] B. A. Arbuzov, M. K. Volkov, and I. V. Zaitsev, Int. J. Mod. Phys. A **24**, 2415 (2009).
[12] B. A. Arbuzov, Eur. Phys. J. C **61**, 51 (2009).
[13] B. A. Arbuzov and I. V. Zaitsev, Int. J. Mod. Phys. A **26**, 4945 (2011).
[14] K. Hagiwara, R. D. Peccei, D. Zeppenfeld, and K. Hikasa, Nucl. Phys. **B282**, 253 (1987).
[15] K. Hagiwara, S. Ishihara, K. Szalapski, and D. Zeppenfeld, Phys. Rev. D **48**, 2182 (1993).
[16] B. A. Arbuzov, Phys. Lett. B **288**, 179 (1992).
[17] LEP Electroweak Working Group, arXiv:hep-ex/0612034v2.
[18] H. Bateman and A. Erdélyi, *Higher Transcendental Functions* (McGraw-Hill, New York, Toronto, London, 1953), volume 1.
[19] T. Aaltonen *et al.* (CDF Collaboration), Phys. Rev. Lett. **106**, 171801 (2011); arXiv:1104.0699.
[20] B. A. Arbuzov and I. V. Zaitsev, Int. J. Mod. Phys. A **27**, 1250012-1 (2012).
[21] E. Boos *et al.* (CompHEP Collaboration), Nucl. Instrum. Methods Phys. Res., Sect. A **534**, 250 (2004).
[22] G. Aad *et al.* (ATLAS Collaboration), Phys. Rev. Lett. **108**, 111803 (2012); arXiv:1202.1414.
[23] S. Chatrchyan *et al.* (CMS Collaboration), arXiv:1202.1487.
[24] G. Aad *et al.* (ATLAS Collaboration), Phys. Lett. B **710**, 383 (2012).
[25] S. Chatrchyan *et al.* (CMS Collaboration), Phys. Rev. Lett. **108**, 111804 (2012).
[26] J. S. Gainer *et al.*, arXiv:1112.1405.
[27] H. E. Haber, G. L. Kane, and T. Sterling, Nucl. Phys. **B161**, 493 (1979).
[28] J. F. Gunion, R. Vega, and J. Wudka, Phys. Rev. D **42**, 1673 (1990).